Natural Resources for Human Health

visagaa publishing house

Original Research

View Article online

Check for updates

Received 19 April 2026
Revised 28 April 2026
Accepted 16 June 2026
Available Online 02 September 2026

Edited by Mohmed Isaqali Karobari

KEYWORDS:
Meloxicam
Drug Delivery Systems
Transdermal, Polymers
Drug Compounding
Skin Absorption
In Vitro Techniques

Natr Resour Human Health 2026; 6 (4): 472–483
https://doi.org/10.53365/nrfhh/224638
eISSN: 2583-1194

Formulation and In Vitro Evaluation of Meloxicam-Loaded Transdermal Patches: Effect of Polymeric Blends on Drug Release and Kinetics

Ameen M. Alwossabi[1,2], Imad M. Taj Eldin[1,3], Ahmed M. S. Al-Ghani[1], Mohammed Abdelrahman[4], Ahmed Ashour[5*], Wadah Osman[5], Mohammed Hamed Alqarni[5], Ahmed I. Foudah[5], Mohamed A. El-Sakhawy[6], Reham M. Samra[7]

[1]Department of Pharmacy, Faculty of Medicine and Health Science, AL-Razi University, Sana'a, Yemen
[2]Department of Pharmaceutics, Faculty of Clinical Pharmacy, Hodiedah University, Hodiedah, Yemen
[3]Department of Pharmacology, Faculty of Pharmacy, University of Gezira, Wad Medani, Sudan
[4]Department of Pharmaceutics, Faculty of Pharmacy, University of Gezira, Wad Medani, Sudan
[5]Department of Pharmacognosy, Faculty of Pharmacy, Prince Sattam Bin Abdulaziz University, 11942, Al-Kharj, Saudi Arabia
[6]Department of Medical Laboratory, College of Applied Medical Sciences, Prince Sattam bin Abdulaziz University, Al-Kharj 11942, Saudi Arabia
[7]Department of Pharmacognosy, Faculty of Pharmacy, Mansoura University, Mansoura 35516, Egypt

ABSTRACT: **Background:** Orally administered meloxicam is associated with gastrointestinal adverse reactions and variable bioavailability due to first-pass metabolism. Transdermal drug delivery systems (TDDS) offer a promising alternative because they enable prolonged drug release and enhanced therapeutic efficacy. **Objective:** The current study aimed to develop and evaluate meloxicam-loaded transdermal patches using different polymeric blends to optimize their physicochemical characteristics and drug release behavior. **Methods:** Meloxicam transdermal patches were prepared by the solvent evaporation method using hydroxypropyl methylcellulose (HPMC) in combination with either polyvinyl alcohol (PVA) or polyvinylpyrrolidone (PVP). Six formulations (F1–F6) were evaluated for thickness, weight variation, folding endurance, expansion index, surface pH, drug content uniformity, and in vitro drug diffusion using phosphate buffer (pH 7.4). Drug–polymer compatibility was evaluated using Fourier transform infrared spectroscopy (FTIR). Drug release kinetics were analyzed using mathematical models. Statistical analysis using one-way ANOVA followed by Tukey's test demonstrated significant formulation-dependent differences ($p < 0.05$). **Results:** All formulations exhibited acceptable physicochemical characteristics and a surface pH compatible with skin application. Among the tested formulations, F1 (HPMC:PVA, 3:1) demonstrated the highest cumulative drug release (92% over 12 h), along with good drug content uniformity and

* Corresponding author.
E-mail address: ahmedadelashour@yahoo.com (Ahmed Ashour)

stable mechanical properties. FTIR analysis confirmed the absence of chemical interactions between meloxicam and the polymers. Kinetic modeling indicated that drug release predominantly followed diffusion-controlled and non-Fickian mechanisms. **Conclusion:** The optimized formulation (F1) demonstrated favorable performance as a matrix-type transdermal patch for sustained meloxicam delivery. These findings highlight the influence of polymeric composition on drug release behavior and support the potential of transdermal systems as an alternative to oral meloxicam therapy.

1. INTRODUCTION

Transdermal drug delivery systems (TDDS) represent an established alternative to conventional oral and parenteral dosage forms, particularly for drugs requiring prolonged therapy. By enabling controlled drug transport across the skin, TDDS avoid gastrointestinal degradation and hepatic first-pass metabolism, thereby improving systemic availability and minimizing dose-dependent adverse effects. Additional advantages include sustained plasma drug levels, improved patient adherence, reduced dosing frequency, and the ability to terminate therapy by removing the patch when necessary (Chourasia et al., 2019; Sravanthi et al., 2020).

Non-steroidal anti-inflammatory drugs (NSAIDs) remain a cornerstone in the management of pain and inflammatory disorders such as arthritis and musculoskeletal conditions. However, chronic oral administration of NSAIDs is frequently associated with gastrointestinal irritation, ulceration, and systemic toxicity, largely attributable to repeated dosing and high peak plasma concentrations. These limitations highlight the need for alternative drug delivery strategies capable of maintaining therapeutic efficacy while reducing systemic exposure (Beale et al., 2010; Mahajan et al., 2018).

Meloxicam is a preferential cyclooxygenase-2 (COX-2) inhibitor widely prescribed for the treatment of inflammatory and degenerative joint diseases. Despite its clinical usefulness, oral meloxicam therapy is associated with gastrointestinal discomfort and variable bioavailability. Delivering meloxicam via the transdermal route may mitigate these drawbacks by providing sustained systemic drug delivery, minimizing peak-related adverse effects, and enhancing therapeutic consistency (Di Costanzo and Angelico, 2019).

Among TDDS designs, matrix-type transdermal patches are particularly attractive due to their simplicity, stability, and ease of fabrication. In these systems, the drug is homogeneously dispersed within a polymeric matrix that governs hydration, mechanical integrity, and drug diffusion. The choice and ratio of polymers critically influence patch performance, including swelling behavior, flexibility, drug entrapment efficiency, and drug release kinetics. Hydrophilic polymers such as hydroxypropyl methylcellulose (HPMC), polyvinyl alcohol (PVA), and polyvinylpyrrolidone (PVP) are commonly employed because of their film-forming capability, biocompatibility, and ability to modulate drug transport through hydrated polymer networks (Siepmann and Siepmann, 2016).

The present study was designed to develop meloxicam-loaded transdermal patches using different combinations of HPMC with PVA or PVP. The effect of polymeric composition on physicochemical characteristics, in vitro drug diffusion, and release kinetics was systematically evaluated to identify an optimized formulation suitable for sustained transdermal delivery of meloxicam. This study focused on HPMC–PVA and HPMC–PVP blends as model hydrophilic polymer systems because of their film-forming capability, biocompatibility, widespread use in TDDS, and suitability for comparative evaluation. Other natural and synthetic polymers, such as chitosan, ethyl cellulose, Eudragit, carbopol, or composite polymer networks, may exhibit different diffusion and mechanical properties and warrant future investigation.

2. MATERIALS AND METHODS

2.1. Materials

Meloxicam was obtained from Shifaco (Yemen). Hydroxypropyl methylcellulose (HPMC) was purchased from Phre Chemical (India), polyvinylpyrrolidone (PVP K30) from Uni-Chemical (India), and polyvinyl alcohol (PVA) was procured from a local market. Sodium lauryl sulfate (SLS) and propylene glycol (PG) were obtained from Pure Chemical (India). Nutrient agar was supplied by HiMedia (India), while sodium chloride and sodium dihydrogen phosphate were obtained from Pure Chemical (India) and WINLAP (UK), respectively.

Dichloromethane (DCM) and methanol were purchased from SRL (India). Distilled water was supplied by AZHA Pharma (Yemen). Additional laboratory materials

included UV cuvettes, a pH meter, and a micrometer from Mettler Toledo (China); Petri dishes from Glass Co. (India); and pH indicator paper from Hydrion (China). Modified Franz diffusion cells and magnetic stir bars were also used. Instrumentation included a UV-Visible spectrophotometer (Shanghai Sunny, China), a dissolution system (Laboa, China), a magnetic heating stirrer (Labtex, China), and a digital micrometer screw gauge (Real Instrument, China).

2.2. Methods

2.2.1. UV–visible spectrophotometric analysis of meloxicam

Quantitative estimation of meloxicam was carried out using UV-Visible spectrophotometry. A primary stock solution was prepared by dissolving meloxicam in 0.1 N sodium hydroxide, followed by appropriate dilution with distilled water to obtain a series of working solutions. The absorption spectrum was recorded over a wide wavelength range to identify the characteristic absorption maximum. All subsequent measurements were performed at the selected wavelength, and a calibration curve was generated to establish the relationship between concentration and absorbance (Chaudhary et al., 2018).

2.2.2. FTIR compatibility assessment

To investigate possible physicochemical interactions between meloxicam and the selected polymers, Fourier transform infrared spectroscopy (FTIR) was employed. Samples of the pure drug, individual polymers, and their physical mixtures were prepared as potassium bromide discs and analyzed over a broad spectral range. Samples were scanned over the range of 4000–400 cm^{-1}. The resulting spectra were examined for changes in characteristic functional group peaks to assess molecular compatibility within the formulation matrix (Iqbal et al., 2020).

2.2.3. Preparation the transdermal patches of Meloxicam TDP

Calculations dose of drug (Mahajan et al., 2018)

The estimated partition factor of meloxicam

$$(\log P)_{app} = \frac{0.1 \text{ in n-octanol}}{\text{buffer pH7.4}}$$

$$\log K_p(\text{cm/hour}) = -2.72 + 0.7\log K_{oct} - 0.0061MW$$

log Kow = 3.54, The molecular weight is 351.4., water solubility = 22 mg/ml.

Flux = Kp × Sw. So, Flux= 3.54 x 0.022 = 0.7788

Dose = flux × area of patch (cm^2) × time for duration of release (hr)

Where:
Area of patch = 6.25 cm^2
Time required for drug release = 12 h
Dose = 0.7788 x 6.25 x 12 = 58.41mg/6.25 cm^2
Area of film spread = 78.5 cm^2
Dose loaded = 733.6 mg/78.5 cm^2

2.2.4. Preparation of meloxicam transdermal patches

Transdermal patches were fabricated using the solvent evaporation method. Polymeric matrices were prepared by dissolving HPMC in combination with either PVA or PVP in suitable solvents selected according to the solubility characteristics of the polymers. Meloxicam was dissolved separately and incorporated into the polymeric solution along with propylene glycol and sodium lauryl sulfate. The resulting dispersion was mixed thoroughly to ensure the uniform distribution of all components. The homogeneous solution was cast onto flat glass surfaces and allowed to dry under controlled ambient conditions. After complete solvent removal, the formed films were carefully detached and stored under desiccated conditions until further evaluation (Shafique et al. 2021). Table 3 shows the different formulations of the meloxicam transdermal patches.

2.2.5. Evaluation of patch characteristics

2.2.5.1. Physical appearance and thickness

Prepared films were visually examined for surface uniformity, flexibility, and transparency. Thickness measurements were performed at multiple locations using a digital micrometer, and the average values were calculated (Shafique et al. 2021).

2.2.5.2. Mechanical strength

Folding endurance was evaluated by repeatedly folding each patch at the same location until structural failure occurred. The number of folds sustained before rupture was recorded (Shafique et al. 2021).

2.2.5.3. Weight uniformity

Individual patches were weighed using an analytical balance to assess the uniformity of the formulation and casting process (Shafique et al. 2021).

2.2.5.4. Swelling behavior

Patch samples were exposed to phosphate buffer (pH 7.4) to evaluate their hydration characteristics. The extent of swelling was determined by measuring the change in weight over a defined period (Mann et al., 2022).

2.2.5.5. Surface pH

To assess skin compatibility, hydrated patches were placed on buffered agar surfaces, and the surface pH was measured using pH indicator strips (Shafique et al. 2021).

2.2.5.6. Drug content uniformity

Drug content was determined by dissolving defined sections of each patch in suitable solvent systems, followed by spectrophotometric analysis. The results were expressed as the percentage of drug content relative to the theoretical value (Shafique et al. 2021).

2.2.6. In vitro drug diffusion study

The release behavior of meloxicam from the prepared patches was evaluated using a diffusion cell assembly. A hydrated dialysis membrane was mounted between the donor and receptor compartments. Patch samples were placed in the donor compartment, while the receptor compartment contained phosphate buffer maintained at physiological temperature and continuously agitated. Aliquots were withdrawn from the receptor medium at predetermined time intervals and replaced with fresh buffer to maintain sink conditions. The amount of meloxicam diffused was quantified by spectrophotometric analysis, and cumulative drug release profiles were constructed (Rafique et al., 2016).

2.2.7. Kinetic analysis of drug release

The in vitro release data were analyzed using established mathematical models to elucidate the mechanism of drug release. Correlation coefficients were used to evaluate the goodness of fit of each kinetic model, enabling the interpretation of the contributions of diffusion and polymer relaxation to meloxicam release.

2.3. Statistical analysis

All experiments were conducted in triplicate (n = 3), and the results are expressed as the mean ± standard deviation. Statistical comparisons among the formulations were performed using one-way analysis of variance (ANOVA), followed by Tukey's post hoc multiple comparison test, with statistical significance accepted at $p < 0.05$.

3. RESULTS AND DISCUSSIONS

3.1. UV–visible spectrophotometric analysis of meloxicam

After scanning, the λ_{max} of meloxicam was found to be 360 nm. The calibration curve demonstrated a linear

Table 1
Calibration curve of Meloxicam.

Conc. µg/ml	Absorbance at λ = 360 nm
2	0.101
4	0.213
6	0.337
8	0.442
10	0.528
12	0.671

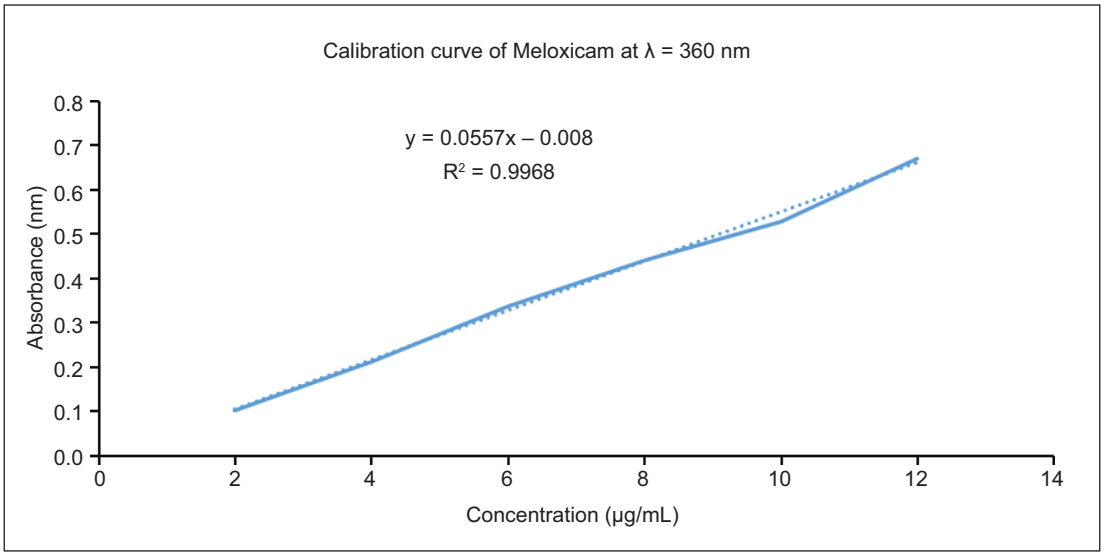

Figure 1. Calibration Curve of Meloxicam at λ = 360 nm.

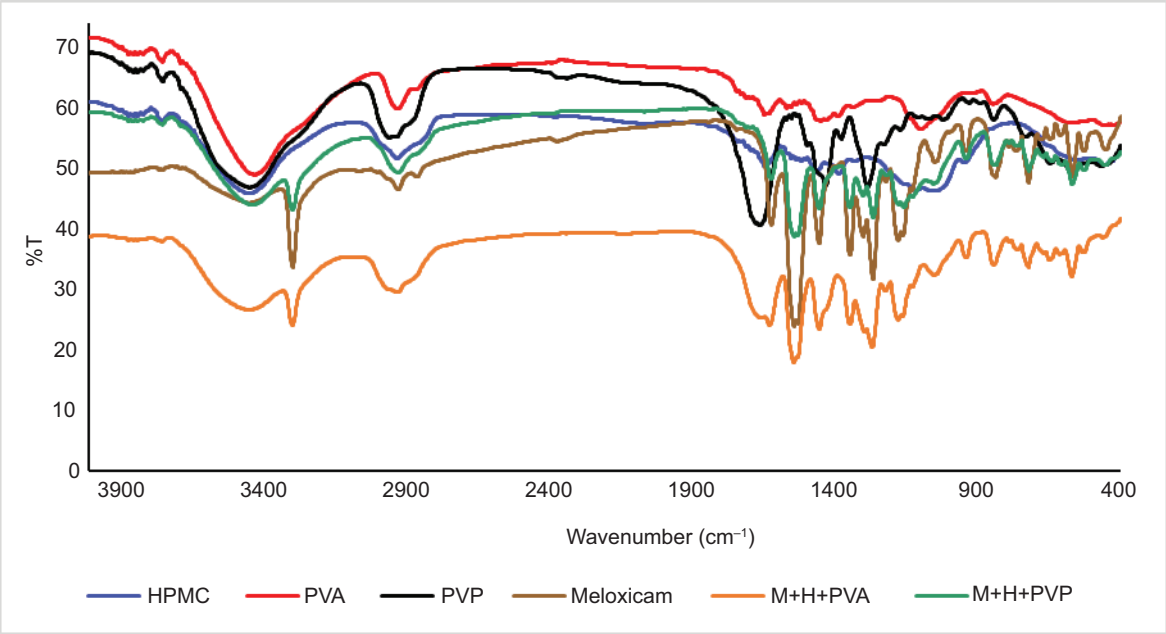

Figure 2. FTIR of Meloxicam, HPMC, PVA, PVP, M+H+PVA, and M+H+PVP

relationship between concentration and absorbance, with an R^2 value of 0.9968 for meloxicam.

3.2. FTIR compatibility assessment results

Fourier Transform Infrared (FTIR) spectroscopy was employed to assess the compatibility of meloxicam with the polymers incorporated into the transdermal patch formulations, namely hydroxypropyl methylcellulose (HPMC), polyvinyl alcohol (PVA), and polyvinylpyrrolidone (PVP). The FTIR spectra of pure meloxicam, the individual polymers, and their corresponding physical mixtures (meloxicam–HPMC–PVA and meloxicam–HPMC–PVP) are illustrated in Fig. (2) (Alburyhi et al., 2025).

The FTIR spectrum of pure meloxicam exhibited distinct absorption bands characteristic of its chemical structure, including a broad peak around 3450 cm^{-1} attributed to O–H stretching, aromatic C–H stretching near 3066 cm^{-1}, aliphatic C–H stretching at approximately 2931 cm^{-1}, a prominent carbonyl stretching band around 1745 cm^{-1}, and aromatic C=C stretching near 1629 cm^{-1}. These absorption bands are consistent with the reported spectral features of meloxicam and confirm the structural integrity of the drug. HPMC exhibited a broad O–H stretching band in the region of 3400 cm^{-1}, along with characteristic ether-related C–O–C stretching vibrations between 1050 and 1150 cm^{-1}. The FTIR spectrum of PVA displayed a broad O–H stretching band around 3300 cm^{-1}, accompanied by a sharp C–H stretching peak near 2940 cm^{-1}. In contrast, PVP exhibited a strong absorption band at approximately 1650 cm^{-1}, corresponding to the carbonyl stretching vibration of its lactam ring (Rowe et al., 2009; Rafique et al., 2016; Thakore SD et al., 2021).

In the spectra of the physical mixtures, all major characteristic peaks of meloxicam and the polymers were clearly retained, with no appearance of new peaks or disappearance of existing peaks. This observation indicates the absence of chemical incompatibility between the drug and the polymeric components. Slight variations in peak intensity and minor band broadening were observed, which may be attributed to weak intermolecular interactions, such as hydrogen bonding, between meloxicam and the polymer chains. Such interactions are commonly associated with improved drug dispersion within polymeric matrices and enhanced physical stability of the formulation (Erxleben, 2016; Zhou et al., 2025). Overall, the FTIR findings confirm that meloxicam remains chemically stable in the presence of HPMC, PVA, and PVP, supporting the suitability of these polymers for use in the transdermal patch system without the risk of drug degradation or adverse chemical interactions.

3.3. Proposed formulations of meloxicam transdermal patches

Table 2 outlines the composition of six different formulations (F1–F6) of meloxicam-loaded transdermal patches developed using the solvent evaporation technique. Each formulation was designed by varying the polymeric matrix

Table 2
Proposed formulations of meloxicam transdermal patches.

Ingredients	F1	F2	F3	F4	F5	F6
	(3:1)	(2:1)	(3:2)	(3:1)	(2:1)	(3:2)
Meloxicam (mg)	733.6	733.6	733.6	733.6	733.6	733.6
HPMC (mg)	3,750	3,750	3,750	3,750	3,750	3,750
PVP (mg)	–	–	–	1,250	1,875	2,500
PVA (mg)	1,250	1,875	2,500	–	–	–
DCM + Methanol (1:2) (ml)	–	–	–	50	50	50
Propylene glycol (mg)	1,000	1,125	1,250	1,000	1,125	1,250
SLS (mg)	100	112.5	125	100	112.5	125
D. Water (mL)	50	50	50	–	–	–

*The above formula gave patch of 78.5 cm^2 area.

components—hydroxypropyl methylcellulose (HPMC), polyvinyl alcohol (PVA), and polyvinylpyrrolidone (PVP)—to investigate their influence on drug release, mechanical integrity, and skin permeation characteristics. All formulations contained a fixed drug loading of 733.6 mg of meloxicam per 78.5 cm^2 of patch area, ensuring uniformity across the test samples. HPMC was consistently included at 3750 mg in all formulations because of its well-established film-forming ability and biocompatibility, which provide mechanical strength and modulate drug release (Kumar et al., 2022). Formulations F1–F3 employed HPMC:PVA blends in ratios of 3:1, 2:1, and 3:2, respectively, whereas F4–F6 were based on HPMC:PVP combinations in similar ratios. PVA was used in F1–F3 as a secondary film-forming agent to enhance flexibility, reduce brittleness, and support drug dispersion (Parhi, 2017). PVP was selected for F4–F6 because of its hydrophilicity and ability to enhance swelling and drug diffusion (Waleka et al., 2021). These blends allowed the comparative evaluation of the mechanical, swelling, and diffusion profiles based on variations in the polymeric matrix. The choice of solvents varied according to polymer solubility. Formulations containing PVA (F1–F3) used distilled water, whereas formulations containing PVP (F4–F6) used a DCM:methanol mixture (1:2) to ensure complete dissolution and homogeneous casting. Propylene glycol (5% of the polymer content) was employed as a plasticizer in all formulations to impart elasticity and reduce brittleness (Siepmann et al., 2016). Sodium lauryl sulfate (SLS) was included at varying concentrations (100–125 mg) as a permeation enhancer to facilitate drug diffusion through the stratum corneum (Dragicevic and Maibech, 2017). The systematic variation in polymer ratios and excipients aimed to optimize critical formulation attributes, such as drug entrapment, patch integrity, hydration/swelling behavior, and transdermal drug flux. By evaluating the effects of PVA and PVP concentrations in combination with HPMC, the study enabled the identification of the most effective matrix composition for controlled meloxicam delivery. After solvent evaporation, the dried residue formed the desired patch, with the drug entrapped within the polymer matrix (Phatale et al., 2022). Transdermal patch systems are generally engineered to deliver the incorporated drug in a controlled and nearly constant manner over an extended period following application to the skin. Such sustained drug delivery is particularly beneficial for the long-term management of chronic disorders, as it helps maintain stable systemic drug levels while minimizing dosing frequency. The effectiveness of transdermal drug transport can be demonstrated by several indicators, including the presence of the drug in the systemic circulation, the identification of the parent compound or its metabolites in excretory fluids, and observable therapeutic outcomes following patch application (Tanwar and Schdeva, 2016).

Evaluation parameters of different formulations of Meloxicam Transdermal Patch

Appearance/Organoleptic Properties

Formulation	Appearance
F1	Light green, soft, flexible
F2	Light green, soft, flexible
F3	Light green, soft, flexible
F4	Light green, soft, flexible
F5	Light green, soft, flexible
F6	Light green, slightly tough

3.4. Evaluation of physicochemical properties of meloxicam transdermal patches

Table 3 summarizes the physicochemical evaluation of six meloxicam transdermal patch formulations (F1–F6) designed with varying ratios of HPMC, PVA, and PVP. The evaluated parameters included physical appearance, thickness, weight variation, folding endurance, swelling index, surface pH, and drug content, all of which are critical for ensuring patch performance, stability, and patient acceptability.

3.4.1. Appearance and thickness

All patches, except F6, exhibited a uniform appearance characterized as light green, soft, and flexible, whereas F6 was slightly tougher, likely because of the higher PVP concentration, which can promote brittle film formation upon solvent evaporation (Dragicevic and Maibech, 2017). Thickness values ranged from 0.33 to 0.40 mm, indicating uniform film casting. Statistical analysis revealed significant differences among the formulations ($p < 0.05$), with F1 exhibiting the

Table 3
Physicochemical evaluation parameters of meloxicam transdermal patches with ANOVA/Tukey multiple comparison grouping.

Parameter	F1	F2	F3	F4	F5	F6
Thickness (mm)	0.400 ± 0.015^{a}	0.330 ± 0.018^{c}	0.330 ± 0.020^{c}	0.340 ± 0.021^{bc}	0.350 ± 0.015^{b}	0.360 ± 0.014^{b}
Weight variation (mg)	716.0 ±3.6^{d}	583.0 ±3.7^{f}	641.0 ±4.4^{e}	1080.0 ±3.8^{b}	919.0 ±3.6^{c}	1163.0 ±4.3^{a}
Folding endurance	60.0 ±1.7^{e}	156.0 ±3.6^{c}	320.0 ±1.7^{a}	250.0 ±2.0^{b}	180.0 ±1.7^{c}	20.0 ±2.0^{f}
Swelling index (%)	122.0 ±4.0^{b}	60.8 ±3.4^{e}	58.4 ±3.1^{e}	86.9 ±3.9^{d}	127.0 ±4.0^{b}	136.0 ±3.5^{a}
Surface pH	6.00 ±0.15^{a}	6.00 ±0.14^{a}	6.00 ±0.18^{a}	6.00 ±0.20^{a}	6.00 ±0.13^{a}	6.00 ±0.16^{a}
Drug content (%)	94.5 ±3.5^{a}	92.6 ±4.3^{ab}	88.2 ±2.6^{c}	92.6 ±2.9^{ab}	91.9 ±3.7^{b}	85.5 ±3.8^{d}

Values are expressed as mean ± SD (n = 3). Within each row, values bearing different superscript letters differ significantly (one-way ANOVA followed by Tukey's post hoc test, $p < 0.05$).

greatest thickness (0.400 ± 0.015 mm^{a}), which was significantly higher than those of F2 and F3 (0.330 ± 0.018–0.020 mm^{c}). F4–F6 exhibited intermediate values (^{b}–^{bc}). Despite these statistically significant differences, the narrow thickness range confirms practical uniformity suitable for transdermal application. The slight increase in thickness with increasing polymer concentration may be attributed to the greater density of the solid polymeric matrix.

3.4.2. Weight uniformity

Patch weight varied significantly among the formulations ($p < 0.05$), ranging from 583 mg (F2^{f}) to 1163 mg (F6^{a}), with each formulation being statistically distinct according to Tukey's grouping. This finding indicates that polymer composition significantly influenced patch mass. In the HPMC:PVA series (F1–F3), increasing the PVA concentration reduced water evaporation and contributed to greater film mass retention, consistent with previous reports on the permeability characteristics of PVA (Patil and Mahapatra, 2016; Patel and Shah, 2018). Similarly, the higher weights of the PVP-rich formulations, particularly F6, may be attributed to the hygroscopic nature of PVP and increased solvent retention. Despite the statistically significant differences, all formulations exhibited acceptable weight uniformity, indicating consistent casting and uniform drug distribution.

3.4.3. Mechanical strength

Folding endurance differed significantly among the formulations ($p < 0.05$) and was strongly influenced by the polymer ratio. F3 exhibited the highest mechanical strength (320 ± 1.7^{a}), which was significantly greater than that of all other formulations, suggesting that the HPMC:PVA (3:2) blend produced optimal elasticity and cohesive strength. F4 ranked second (250 ± 2.0^{b}), whereas F2 and F5 shared the same significance group (156–180^{c}), indicating no significant difference between them. F1 (60 ± 1.7^{e}) and, particularly, F6 (20 ± 2.0^{f}) exhibited significantly lower flexibility. The poor folding endurance of F6 supports the inference that higher PVP levels increase brittleness when not sufficiently plasticized (Sethi and Mazumder, 2018). These statistically significant differences confirm that polymer composition critically governs the mechanical integrity of the patches.

3.4.4. Swelling behavior

The swelling index showed statistically significant differences among the formulations ($p < 0.05$). F6 demonstrated the highest swelling (136 ± 3.5^{a}), which was significantly greater than that of all other formulations, whereas F1 and F5 (122–127%^{b}) were not significantly different from each other. F2 and F3 exhibited the lowest swelling values (^{e}) and were statistically similar. These findings confirm that PVP-rich formulations promote greater hydration because of the hydrophilic nature of the polymer, whereas PVA-containing systems limit water uptake because of their lower water permeability (Kumar et al., 2018; Godbole et al., 2017). The statistical grouping further supports the direct influence of polymer type on swelling-mediated drug diffusion. The moderate swelling observed in F1 may partly explain its superior drug release behavior while maintaining structural stability.

3.4.5. Surface pH

All formulations exhibited surface pH values ranging from 6.0 to 6.5, which are compatible with normal skin physiology. Statistical analysis revealed no significant differences among the formulations (all shared superscript a, $p > 0.05$), confirming that polymer composition did not significantly affect surface pH. This uniformity is desirable, as it suggests a minimal risk of skin irritation and supports the dermatological suitability of the developed patches (Alkilani et al., 2022).

3.4.6. Drug content uniformity:

Drug content ranged from 85.5% (F6[d]) to 94.5% (F1[a]), with statistically significant differences among the formulations ($p < 0.05$). F1 exhibited significantly higher drug content than F3, F5, and F6, indicating superior drug entrapment within the HPMC:PVA matrix. F2 and F4 shared overlapping significance groups ([ab]), suggesting statistically comparable drug-loading efficiency. The lowest drug content observed in F6 may be attributed to drug migration or phase separation associated with higher PVP concentrations (Albertini et al., 2018). These findings support the role of polymer composition in controlling drug retention and matrix homogeneity.

Collectively, the statistical analysis confirmed that polymer composition significantly influenced thickness, weight, folding endurance, swelling behavior, and drug content, whereas surface pH remained unaffected. Among the tested formulations, F1 exhibited the most balanced physicochemical profile, combining significantly higher drug content, favorable

Table 4

Cumulative drug release profiles of formulations F1–F6 over 12 h in phosphate buffer (pH 7.4)

Time (h)	F1	F2	F3	F4	F5	F6
1	26.8±0.65[c]	23.5±0.67[d]	17.5±0.65[e]	30.9±0.75[b]	34.2±0.92[a]	31.4±0.95[b]
2	35.4±0.53[a]	35.5±0.85[a]	34.6±0.62[a]	33.3±0.65[b]	35.5±0.76[a]	35.2±0.90[a]
4	42.1±0.53[c]	41.9±0.85[c]	44.0±0.90[bc]	49.6±1.01[a]	46.2±0.95[b]	44.6±1.05[b]
6	56.9±1.10[c]	58.2±1.31[b]	57.1±1.15[c]	59.1±1.05[ab]	59.6±1.15[a]	56.3±1.15[c]
8	74.6±0.95[a]	70.3±1.11[c]	71.3±1.25[bc]	72.2±1.05[b]	72.5±1.20[b]	64.8±1.36[d]
10	86.9±1.11[b]	83.1±1.05[c]	81.6±1.10[c]	89.5±1.05[a]	88.0±1.25[ab]	81.2±1.05[c]
12	92.0±1.15[a]	86.5±1.45[c]	84.7±1.20[d]	91.2±1.02[a]	89.4±1.36[b]	83.8±1.40[d]

Mean ± SD (n=3); different superscripts within each row indicate significant difference ($p < 0.05$).

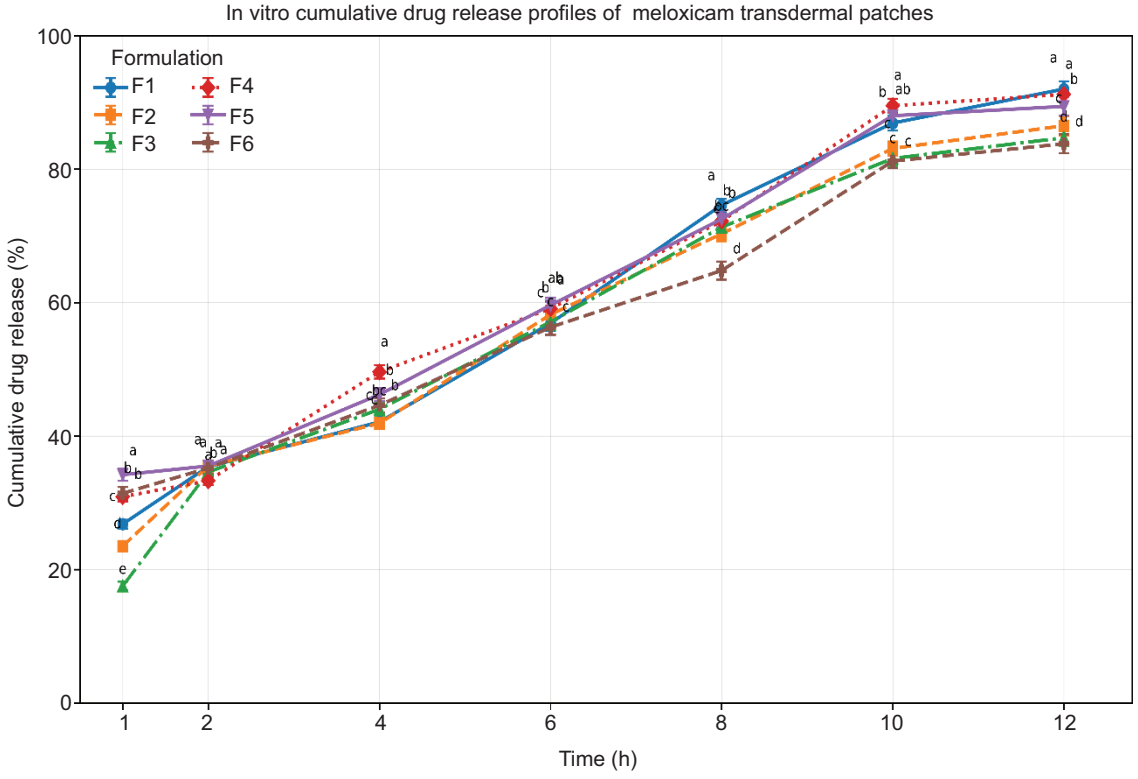

Figure 3. In vitro cumulative drug release profiles of meloxicam transdermal patches (F1–F6) in phosphate buffer (pH 7.4) over 12 h. Data are presented as the mean ± SD (n = 3). Error bars represent the standard deviation. Significant differences among the formulations at each time point were determined using one-way ANOVA followed by Tukey's post hoc test ($p < 0.05$).

swelling behavior, acceptable thickness, and superior drug release performance, despite its lower folding endurance compared with F3. F3 demonstrated significantly greater mechanical strength but lower swelling and drug loading, whereas F6, although exhibiting the highest swelling, was limited by significantly lower flexibility and drug content. These results demonstrate that optimizing the polymer blend ratios is essential for achieving a balance among mechanical integrity, hydration behavior, and drug delivery performance.

3.5. In vitro drug diffusion study

Table 4 and Fig. 3 present the cumulative percentage release of meloxicam from six transdermal patch formulations (F1–F6) over 12 h in phosphate buffer (pH 7.4). All data are expressed as the mean ± SD (n = 3), and differences among the formulations at each sampling time were analyzed using one-way ANOVA followed by Tukey's post hoc test ($p < 0.05$). An initial burst release was observed in all formulations during the first 2 h, which is characteristic of matrix-type transdermal systems because of the rapid release of drug located near the patch surface. At 1 h, statistically significant differences were observed among the formulations ($p < 0.05$), with F5 (34.2 ± 0.92^{a}) exhibiting significantly greater drug release than all other formulations, whereas F3 (17.5 ± 0.65^{e}) exhibited significantly lower drug release. F4 and F6 shared the same significance group (^{b}), indicating comparable early diffusion behavior, whereas F1 (^{c}) and F2 (^{d}) exhibited intermediate release. At 2 h, most formulations (F1, F2, F3, F5, and F6) shared the same significance group (^{a}), indicating no significant differences among them, whereas F4 (33.3 ± 0.65^{b}) exhibited significantly lower drug release, suggesting that early-stage diffusion was governed primarily by hydration and surface drug availability rather than polymer-controlled diffusion resistance. As diffusion progressed, significant formulation-dependent differences became more evident. At 4 h, F4 (49.6 ± 1.01^{a}) exhibited significantly greater drug release than all other formulations, whereas F1 and F2 belonged to the lowest statistical group (^{c}). F3 and F6 were statistically comparable ($^{b–c}$), whereas F5 exhibited intermediate release (^{b}). At 6 h, F5 (59.6 ± 1.15^{a}) exhibited the highest drug release, although it was statistically comparable to F4 (59.1 ± 1.05^{ab}), whereas F1, F3, and F6 belonged to the lower significance groups. These findings indicate that the polymer ratio significantly influenced sustained diffusion kinetics during the matrix hydration phase. For the HPMC:PVA series (F1–F3), increasing the PVA concentration significantly reduced drug release at later time points, particularly in F3, supporting the hypothesis that higher polymer content increases matrix viscosity and diffusional resistance (Dangre et al., 2016; Umaredkar et al., 2020). Significant differences became most pronounced during the sustained-release phase. At 8 h, F1 (74.6 ± 0.95^{a}) exhibited significantly higher drug release than all other formulations, whereas F6 (64.8 ± 1.36^{d}) exhibited significantly lower diffusion. F4 and F5 occupied intermediate significance groups. At 10 h, F4 (89.5 ± 1.05^{a}) exhibited the highest drug release and was statistically comparable only to F5 (88.0 ± 1.25^{ab}), whereas F2, F3, and F6 belonged to significantly lower significance groups (^{c}). At 12 h, F1 (92.0 ± 1.15^{a}) achieved the highest cumulative drug release and was statistically comparable only to F4 (91.2 ± 1.02^{a}), but significantly greater than F5 (89.4 ± 1.36^{b}), F2 (86.5 ± 1.45^{c}), and the lowest-performing formulations, F3 and F6 (^{d}). These findings support the ranking of drug release performance as F1 > F4 > F5 > F2 > F3 > F6. Formulations F1–F3 utilized HPMC:PVA blends, whereas F4–F6 were based on HPMC:PVP systems. The superior performance of F1 (3:1 HPMC:PVA) may be attributed to an optimal balance among matrix swelling, permeability, and structural stability, whereas the significantly lower release observed with F3 suggests that increasing the PVA concentration may have formed a denser, more viscous gel barrier that hindered drug diffusion (Umaredkar et al.,2020). Within the HPMC:PVP formulations, F4 exhibited significantly greater late-stage drug release than F6, confirming that increasing the PVP concentration beyond an optimal level may promote excessive hydration and gel barrier formation, ultimately restricting sustained drug diffusion (Majee et al., 2025; Ramkant et al., 2015). The biphasic release profile, consisting of an initial burst release followed by controlled sustained release, is typical of matrix-controlled systems. Statistical comparisons revealed minimal differences during the initial burst phase but increasingly significant differences at later time points, indicating that polymer composition exerted greater control over sustained drug diffusion than over the initial release. The narrow error bars (±SD) observed throughout the study indicate good reproducibility of the diffusion experiments and support the reliability of the release data. Collectively, these findings demonstrate that optimization of the polymer composition significantly influenced meloxicam release behavior, with F1 providing the most favorable sustained drug release profile while maintaining controlled diffusion kinetics, supporting its selection as the optimized formulation for further in vivo investigation.

3.6. Kinetic analysis of drug release results

The release profiles of all six formulations (F1–F6) were analyzed using Zero-order, First-order, Higuchi, and Korsmeyer–Peppas models to elucidate the mechanism of

Table 5
Comparative kinetic model fitting parameters (R^2) and mechanistic interpretation of meloxicam release from transdermal patches.

Formulation	Zero-order R^2	First-order R^2	Higuchi R^2	Korsmeyer-Peppas R^2	n value	Mechanism
F1	0.984492	0.919965	0.957590	0.970403	0.51	Non-Fickian
F2	0.979966	0.944239	0.974794	0.982257	0.48	Anomalous
F3	0.963273	0.975261	0.972968	0.986480	0.56	Non-Fickian
F4	0.982308	0.910253	0.967795	0.970163	0.52	Anomalous
F5	0.979491	0.864167	0.952709	0.952718	0.49	Anomalous
F6	0.986665	0.854756	0.958042	0.959322	0.45	Near Fickian

Release exponent values (n = 0.45–0.56) further confirmed anomalous/non-Fickian transport.

meloxicam release from the polymeric matrices. The goodness of fit of each model was assessed using the coefficient of determination (R^2), where higher values indicate better agreement between the experimental data and the mathematical model. Zero-order plots showed strong correlation coefficients for all formulations (R^2 = 0.963–0.987), indicating relatively constant release rates over time. Among the formulations, F6 (R^2 = 0.9867) and F1 (R^2 = 0.9845) exhibited the highest Zero-order fits, suggesting more controlled and sustained release behavior. Comparative analysis showed that F6 > F1 > F4 > F2 > F5 > F3 for the Zero-order fit, indicating that formulation composition significantly influenced the maintenance of constant release. The high Zero-order fit observed for F1 supports its statistically superior diffusion behavior observed in Table 4. First-order fitting varied considerably among formulations (R^2 = 0.855–0.975). F3 showed the highest First-order fit (0.9753), markedly greater than those of the other formulations, suggesting that its release was more concentration-dependent. This stronger First-order behavior for F3 is consistent with its comparatively lower cumulative release and denser polymer matrix, where drug release likely depends more strongly on the residual drug concentration within the system. The substantially lower First-order fits of F5 and F6 indicate that First-order kinetics did not adequately describe those formulations. The Higuchi model showed consistently high correlations (R^2 > 0.95) across all formulations, supporting diffusion as a major mechanism of release. F2 exhibited the strongest Higuchi fit (0.9748), followed closely by F3 and F4, suggesting that release from these systems was strongly governed by matrix diffusion. The uniformly high Higuchi correlations quantitatively support the diffusion-controlled behavior observed experimentally and confirm that drug transport through hydrated polymer networks contributed substantially to release. The Korsmeyer–Peppas model produced the highest overall goodness-of-fit values for several formulations, particularly F3 = 0.9865, F2 = 0.9823, and F1 = 0.9704. For F2 and F3, the Korsmeyer–Peppas model provided a better fit than the Zero-order, First-order, and Higuchi models, indicating anomalous transport involving both diffusion and polymer relaxation. The superiority of the Korsmeyer–Peppas fit over the other models for several formulations supports non-Fickian release mechanisms rather than purely concentration-driven or simple diffusion-controlled release. The strong Higuchi and Korsmeyer–Peppas fits suggest that meloxicam release was predominantly governed by diffusion through hydrated polymer matrices combined with polymer relaxation/swelling processes. This interpretation is further supported by the swelling index data, where highly swelling formulations showed corresponding diffusion-controlled behavior. Thus, kinetic modeling and ANOVA-supported release data collectively indicate that polymer composition significantly affected not only the extent of drug release but also the underlying release mechanism. Although the Higuchi and Korsmeyer–Peppas models suggested diffusion-controlled and anomalous transport mechanisms, these mathematical models simplify complex skin transport phenomena and assume idealized conditions. The dialysis membrane-based Franz diffusion model does not fully replicate the structural and barrier properties of human skin; therefore, in vitro diffusion may not directly predict in vivo permeation behavior. Furthermore, kinetic models based on correlation coefficients provide mechanistic indications rather than definitive proof of the release mechanisms. Compared with conventional oral meloxicam, which is associated with gastrointestinal irritation, fluctuating plasma levels, and first-pass metabolism, the optimized transdermal formulation (F1) demonstrated sustained release over 12 h, suggesting the potential to reduce dosing frequency and minimize peak-related adverse effects. Although direct in vivo bioavailability comparison was beyond the scope of this study, the sustained release behavior observed supports the potential therapeutic advantage of transdermal delivery over oral

administration. Selection of the optimized formulation was based on a multi-response criterion incorporating the highest cumulative release, acceptable mechanical integrity, drug content uniformity, favorable swelling behavior, and kinetic suitability. Based on these combined responses, F1 was selected as the optimized formulation.

4. CONCLUSION

This study successfully developed and evaluated meloxicam-loaded transdermal patches utilizing different ratios of HPMC, PVA, and PVP polymers. The physicochemical properties, drug content, and in vitro release performance of the patches varied significantly with polymer composition. Among the tested formulations, F1 (HPMC 3:1) demonstrated the most favorable profile, combining optimal drug release (92% over 12 h), consistent physical attributes, and good mechanical integrity. Kinetic modeling of the drug release profiles revealed that the Korsmeyer–Peppas and Higuchi models provided the best fit for most formulations, indicating a predominance of diffusion-controlled and non-Fickian release mechanisms. Formulation F3 showed First-order kinetics, suggesting concentration-dependent release. The highest R^2 values obtained from the Korsmeyer–Peppas model highlight the significance of both diffusion and polymer relaxation/swelling in controlling meloxicam release. Overall, the findings affirm that the selection and ratio of polymers play a crucial role in modulating drug diffusion, mechanical properties, and transdermal delivery efficiency. F1 stands out as a promising formulation for further in vivo evaluation and potential clinical application in sustained-release therapy for conditions requiring prolonged NSAID administration. Compared with conventional oral meloxicam, transdermal delivery may reduce gastrointestinal irritation, avoid first-pass metabolism, minimize peak-trough plasma fluctuations, and provide sustained drug input. While oral meloxicam exhibits variable systemic exposure and NSAID-associated gastrointestinal adverse effects, the optimized transdermal formulation (F1) may offer a potential alternative sustained-delivery platform. Future optimization may explore broader polymeric systems and hybrid matrices to further improve transdermal performance.

ACKNOWLEDGMENT

The authors extend their appreciation to Prince Sattam bin Abdulaziz University for funding this research work through the project number (PSAU/2025/01/38777).

AUTHORS' CONTRIBUTIONS

A.M.A., I.M.T.E., and A.M.S.A-G.: experiments, interpretation and writing. M.A.: experiments, review, interpretation of results and review. A.A., W.O., M.H.A., A.I.F., M.A.E-S., and R.M.S.: Writing – review & editing. All authors have reviewed and approved the final version of the manuscript and take full responsibility for its content. The authors confirm that no paper mill and artificial intelligence was used.

ORCID

Ameen M. Alwossabi	0000-0002-4373-0332
Imad M. Taj Eldin	0000-0002-4230-952X
Ahmed M. Al-Ghani	0000-0001-8761-5662
Mohammed Abdelrahman	0009-0003-3077-4525
Ahmed Ashour	0000-0003-4081-0369
Wadah Osman	0000-0003-4368-5161
Mohammed Hamed Alqarni	0000-0002-7061-9111
Ahmed I. Foudah	0000-0002-6728-8614
Mohamed Abdel-Monem El- Sakhawy	0000-0001-9494-339X
Reham M. Samra	0000-0003-0348-8817

REFERENCES

Albertini, B., Melegari, C., Bertoni, S., Dolci, L.S., Passerini, N. 2018. A novel approach for dry powder coating of pellets with ethylcellulose. Part II: Evaluation of caffeine release. AAPS PharmSciTech. 19(3), 1426–1436. https://doi.org/10.1208/s12249-018-0964-9.

Alburyhi, M.M., Noman, M.A., Saif, A.A. 2025. Formulation and evaluation of meloxicam emulgel delivery system for topical applications. World J Pharm Res. 14(4), 1324–1337. https://doi.org/10.20959/wjpr20254-35702.

Alkilani, A.Z., Nasereddin, J., Hamed, R., Nimrawi, S., Hussein, G., Abo-Zour, H., Donnelly, R.F. 2022. Beneath the skin: A review of current trends and future prospects of transdermal drug delivery systems. Pharmaceutics. 14(6), 1152. https://doi.org/10.3390/pharmaceutics14061152.

Beale, J.M., Block, J.H., Hill, R. 2010. Organic medicinal and pharmaceutical chemistry. Philadelphia: Lippincott Williams & Wilkins.

Chaudhary, K,B,, Bhardwaj, K., Verma, G., Kumar, P. 2018. Validated analytical method development for the determination of meloxicam by UV spectroscopy in API and pharmaceutical dosage form. Asian J Pharm Educ Res. 7(2), 60–69.

Chourasia, S., Shukla, T., Dangi, S., Upmanyu, N., Jain, N. 2019. Formulation and evaluation of matrix transdermal patches of meloxicam. J Drug Deliv Ther. 9(1-S), 209–213. https://doi.org/10.22270/jddt.v9i1-s.2326

Dangre, P.V., Godbole, M.D., Ingale, P.V., Mahapatra, D.K. 2016. Improved dissolution and bioavailability of eprosartan mesylate formulated as solid dispersions using conventional methods.

Indian J Pharm Educ Res. 50(Suppl 2), S209–S217. https://doi.org/10.5530/ijper.50.2.9.

Di Costanzo, A., Angelico, R. 2019. Formulation strategies for enhancing the bioavailability of silymarin: The state of the art. Molecules. **24**(11), 2155. https://doi.org/10.3390/molecules24112155

Dragicevic, N., Maibach, H.I. 2017. editors. *Percutaneous Penetration Enhancers: Physical Methods in Penetration Enhancement*. Berlin: Springer. https://doi.org/10.1007/978-3-662-53270-6

Erxleben, A. 2016. Application of vibrational spectroscopy to study solid-state transformations of pharmaceuticals. Curr Pharm Des. 22(32), 4883–4911. https://doi.org/10.2174/1381612822666160607071445

Godbole, M.D., Mahapatra, D.K., Khode, P.D. 2017. Fabrication and characterization of edible jelly formulation of stevioside: A nutraceutical or OTC aid for the diabetic patients. Inventi Rapid Nutraceuticals. (2), 1–9.

Iqbal, A., Hossain, S., Shamim, A., Islam, M., Siddique, A.T. 2020. Formulation, in vitro evaluation and characterization of atorvastatin solid dispersion. Trop J Pharm Res. 19(6), 1131–1138. https://doi.org/10.4314/tjpr.v19i6.2.

Kumar, B., Pandey, M., Aggarwal, R., Sahoo, P.K. 2022. A comprehensive review on invasomal carriers incorporating natural terpenes for augmented transdermal delivery. Futur J Pharm Sci. 8, 50. https://doi.org/10.1186/s43094-022-00417-5

Kumar, L., Verma, S., Singh, M., Chalotra, T., Utreja, P. 2018. Advanced drug delivery systems for transdermal delivery of non-steroidal anti-inflammatory drugs: A review. Curr Drug Deliv. 15(8), 1087–1099. https://doi.org/10.2174/1567201815666180618101659.

Mahajan, N.M., Zode, G.H., Mahapatra, D.K., Thakre, S., Dumore, N., Gangane, P.S. 2018. Formulation development and evaluation of transdermal patch of piroxicam for treating dysmenorrhoea. J Appl Pharm Sci. 8(11), 35–41. https://doi.org/10.7324/JAPS.2018.81105

Majee, S.B, Gupti, S., Mishra, T., Bera, R. 2025. *In vitro*, *ex vivo* and *in vivo* studies on anti-hypertensive-loaded transdermal and buccal patches. J Drug Deliv Ther. 15(4).

Mann, G., Gurave, P.M., Kaul, A., Kadiyala, K.G., Pokhriyal, M., Srivastava, R.K., Kumar, A., Datta, A. 2022. Polymeric and electrospun patches for drug delivery through buccal route: Formulation and biointerface evaluation. J Drug Deliv Sci Technol. 68:103030. https://doi.org/10.1016/j.jddst.2021.103030.

Parhi, R. 2017. Cross-linked hydrogel for pharmaceutical applications: A review. Adv Pharm Bull. 7(4), 515–530. https://doi.org/10.15171/apb.2017.061

Patel, A.V., Shah, B.N. 2018. Transdermal drug delivery system: A review. Pharma Sci Monit. 9(2).

Patil, M.D., Mahapatra, D.K., Dangre, P.V. 2016. Formulation and *in vitro* evaluation of once-daily sustained release matrix tablet of nifedipine using rate retardant polymers. Inventi Impact Pharm Tech. (4), 190–196.

Phatale, V., Vaiphei, K.K., Jha, S., Patil, D., Agrawal, M., Alexander, A. 2022. Overcoming skin barriers through advanced transdermal drug delivery approaches. J Control Release. 351, 361–380. https://doi.org/10.1016/j.jconrel.2022.09.049

Rafique, A., Zia, K.M., Zuber, M., Tabasum, S., Rehman, S. 2016. Chitosan functionalized poly(vinyl alcohol) for prospects biomedical and industrial applications: A review. Int J Biol Macromol. 87, 141–154. https://doi.org/10.1016/j.ijbiomac.2016.02.035.

Ramkanth, S., Jayaprakash, S., Vimalakannan, T. 2015. Formulation and evaluation of monolithic drug-in-adhesive type patch containing tenoxicam. Int J Pharm Sci Res. 6(2), 654–659.

Rowe, R.C., Sheskey, P.J., Quinn, M.E. 2009. editors. Handbook of pharmaceutical excipients. 6th ed. London: Pharmaceutical Press. ISBN: 9781582121352.

Sethi, B., Mazumder, R. 2018. Comparative evaluation of selected polymers and plasticizer on transdermal drug delivery system. Int J App Pharm. 10(4), 67–73. https://doi.org/10.22159/ijap.2018v10i4.25661.

Shafique, N., Siddiqui, T., Zaman, M., Iqbal, Z., Rasool, S., Ishaque, A., Siddique, W., Alvi, M.N. 2021. Transdermal patch, co-loaded with pregabalin and ketoprofen for improved bioavailability; *in vitro* studies. Polym Compos. 29(9 Suppl), S376–S388. https://doi.org/10.1177/096739111211004516.

Siepmann, J., Siepmann, F., Paeratakul, O., Bodmeier, R. 2016. Factors affecting drug release from pellets coated with the ethylcellulose-pseudolatex Aquacoat®. In: McGinity JW, editor. *Aqueous Polymeric Coatings for Pharmaceutical Dosage Forms*. 3rd ed. Boca Raton (FL): CRC Press. p. 177–194. https://doi.org/10.1201/9781420000016

Siepmann, J., Siepmann, F. 2016. Time-controlled drug delivery systems. In: Florence AT, Siepmann J, editors. *Modern Pharmaceutics. Volume 2: Applications and Advances*. 5th ed. Boca Raton (FL): CRC Press. p. 19–40. https://doi.org/10.1201/b19147-2

Sravanthi, K., Reddy, D.R.B., Sirisha, A., Pavani, A., Lakshmi, B.K., Sowjanya, B. 2020. Preparation and in vitro evaluation of transdermal patch of aceclofenac. Am J Pharmtech Res. 10(2). https://doi.org/10.46624/ajptr.2020.v10.i2.014

Tanwar, H., Sachdeva, R. 2016. Transdermal drug delivery system: A review. Int J Pharm Sci Res. 7(6), 2274–2290. https://doi.org/10.13040/IJPSR.0975-8232.7(6).2274-90

Thakore, S.D., Akhtar, J., Jain, R., Paudel, A., Bansal, A.K. 2021. Analytical and computational methods for the determination of drug-polymer solubility and miscibility. Mol Pharm. 18(8), 2835–2866. https://doi.org/10.1021/acs.molpharmaceut.1c00141

Umaredkar, A.A., Dangre, P.V., Mahapatra, D.K., Dhabarde, D.M. 2020. Fabrication of chitosan-alginate polyelectrolyte complexed hydrogel for controlled release of cilnidipine: A statistical design approach. Mater Technol. 35(11), 697–707. https://doi.org/10.1080/10667857.2019.1689893

Waleka, E., Stojek, Z., Karbarz, M. 2021. Activity of povidone in recent biomedical applications with emphasis on micro- and nano drug delivery systems. Pharmaceutics. 13(5), 654. https://doi.org/10.3390/pharmaceutics13050654

Zhou, W., Han, M., Zhang, H., Zhang, T., Tian, H., Yang, T., Liu, T. 2025. Effect of PVP and HPMC on production of indomethacin amorphous nanoparticles: Experiments and molecular dynamics simulations. Drug Dev Ind Pharm. 51(6), 622–633. https://doi.org/10.1080/03639045.2025.2495136.